Status of the MUSE experiment
with a focus on radiative corrections

Steffen Strauch
University of South Carolina

for the MUSE Collaboration

Supported in parts by the U.S. National Science Foundation: NSF PHY-2111050. The MUSE experiment is supported by the U.S. Department of Energy, the U.S. National Science Foundation, the Paul Scherrer Institute, and the US-Israel Binational Science Foundation.

NSTAR 2022, Santa Margherita Ligure, Oct 17 – 21, 2022

MUon Scattering Experiment (MUSE) at PSI

Direct test of μp and ep interactions in a scattering experiment:

- higher precision than previously for μp,
- low-Q^2 region for sensitivity to the **proton charge radius**, Q^2 = 0.002 to 0.07 GeV^2,
- with μp and ep to have direct **μ/e comparison**,
- with μ^+, μ^- and e^+, e^- to study possible **2γ mechanisms**.

MUSE

$$e^- p \rightarrow e^- p$$
$$e^+ p \rightarrow e^+ p$$
$$\mu^- p \rightarrow \mu^- p$$
$$\mu^+ p \rightarrow \mu^+ p$$

The MUon Scattering Experiment at PSI (MUSE), MUSE Technical Design Report, arXiv:1709.09753 [physics.ins-det].

Projected MUSE proton charge-radius results

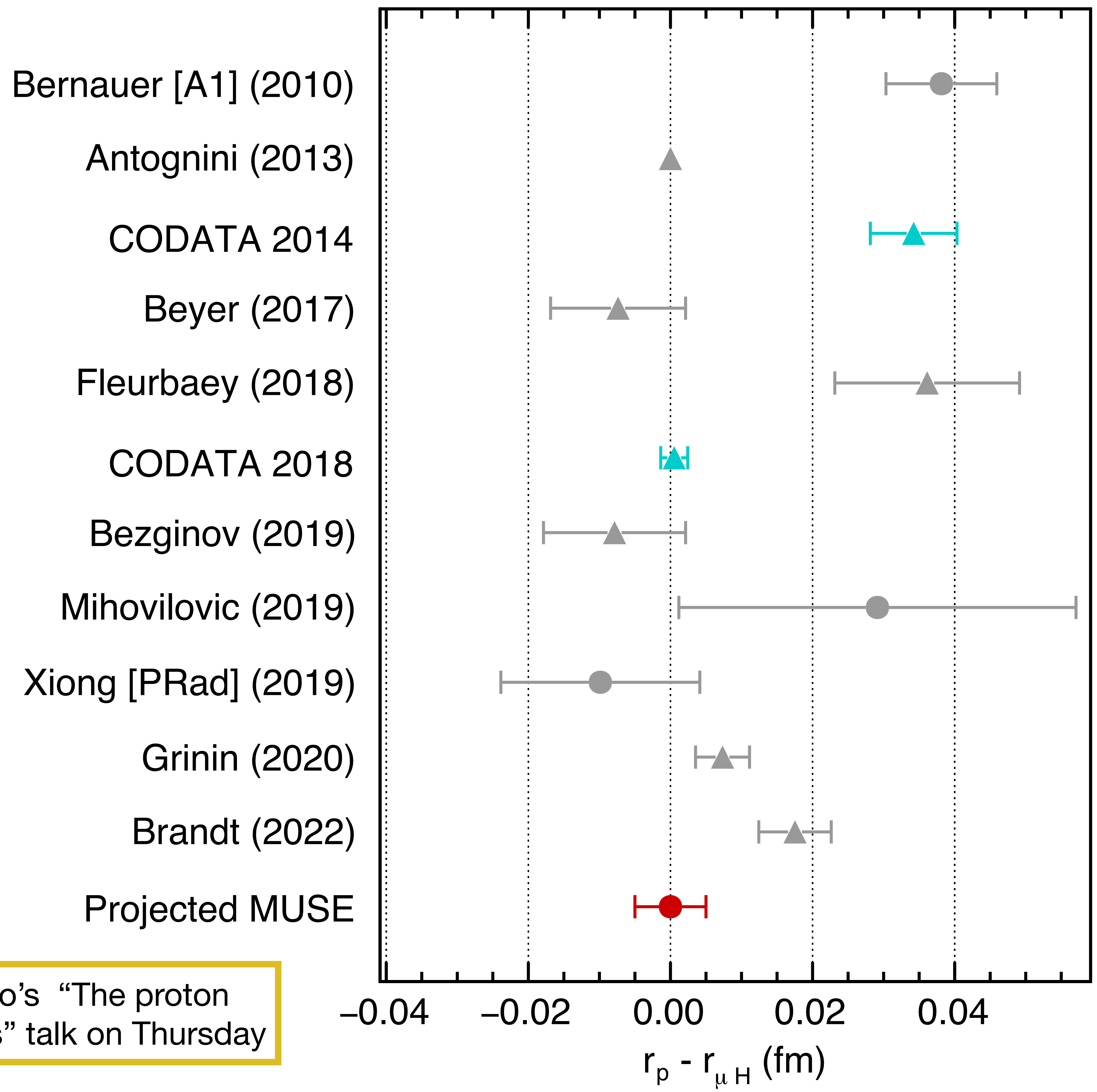

→ Haiyan Gao's "The proton charge radius" talk on Thursday

What is the radius?

Absolute values of extracted e/μ radii (assuming no +/- difference seen):

$\sigma(r_e)$, $\sigma(r_\mu) \approx 0.008$ fm

How different are the e/μ radii?

(truncation error largely cancels)

Sensitivity to differences in extracted e/μ radii:

$\sigma(r_e - r_\mu) \approx 0.005$ fm

Comparisons of **e to μ** or of **positive to negative** are insensitive to many of the systematics

The MUon Scattering Experiment at PSI (MUSE), MUSE Technical Design Report, arXiv:1709.09753 [physics.ins-det].

Anticipated e and μ data for G_E from MUSE

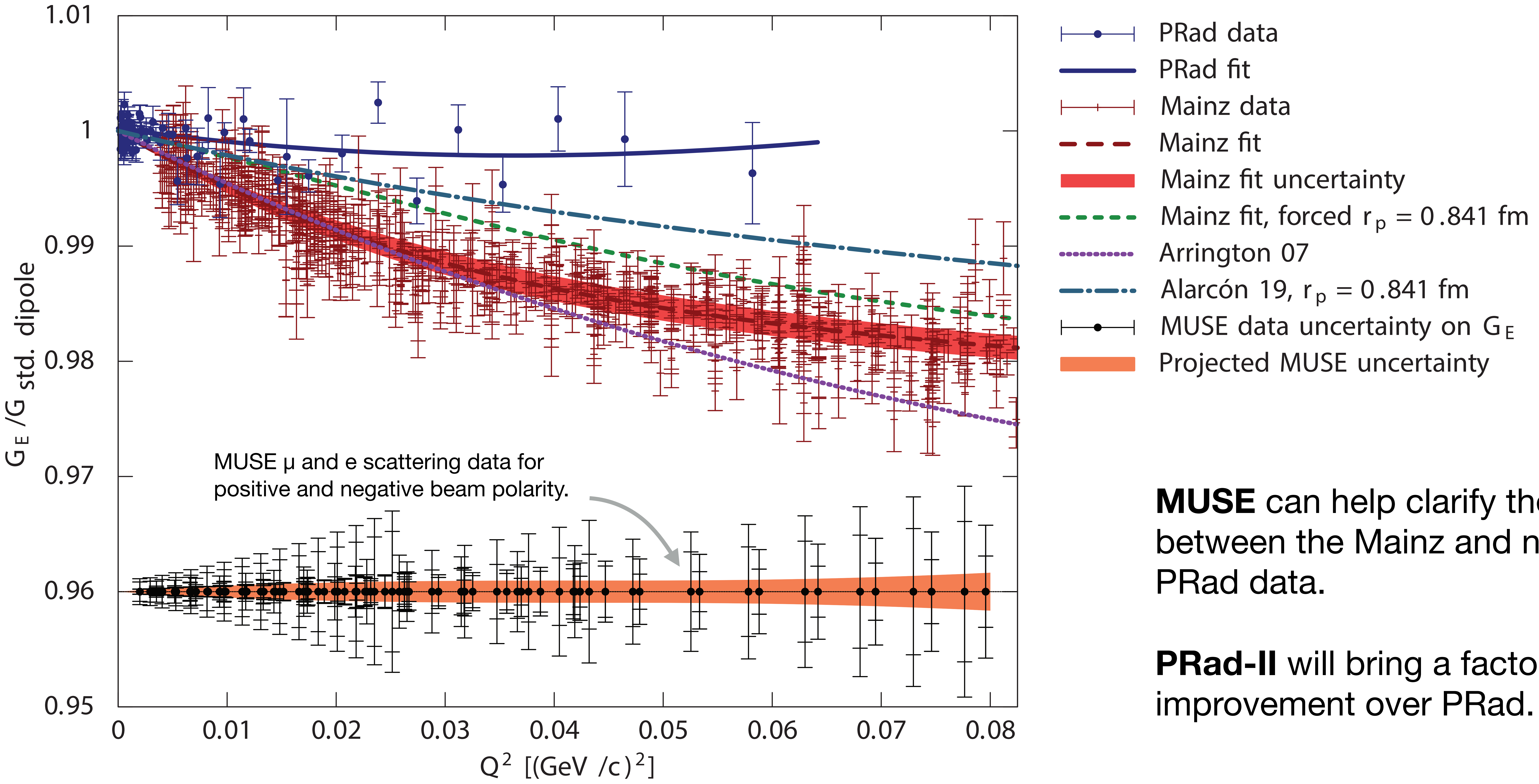

MUSE can help clarify the tension between the Mainz and new PRad data.

PRad-II will bring a factor of 4 improvement over PRad.

E. Cline, et al., SciPost Phys. Proc. 5, 023 (2021)

MUSE allows to study two-photon exchange

Projected relative uncertainty in the ratio of μ^+p to μ^-p elastic cross sections. Systematics: 0.2% in the cross section ratio (0.1% in $\delta_{2\gamma}$).

The MUon Scattering Experiment at PSI (MUSE), MUSE Technical Design Report, arXiv:1709.09753 [physics.ins-det].

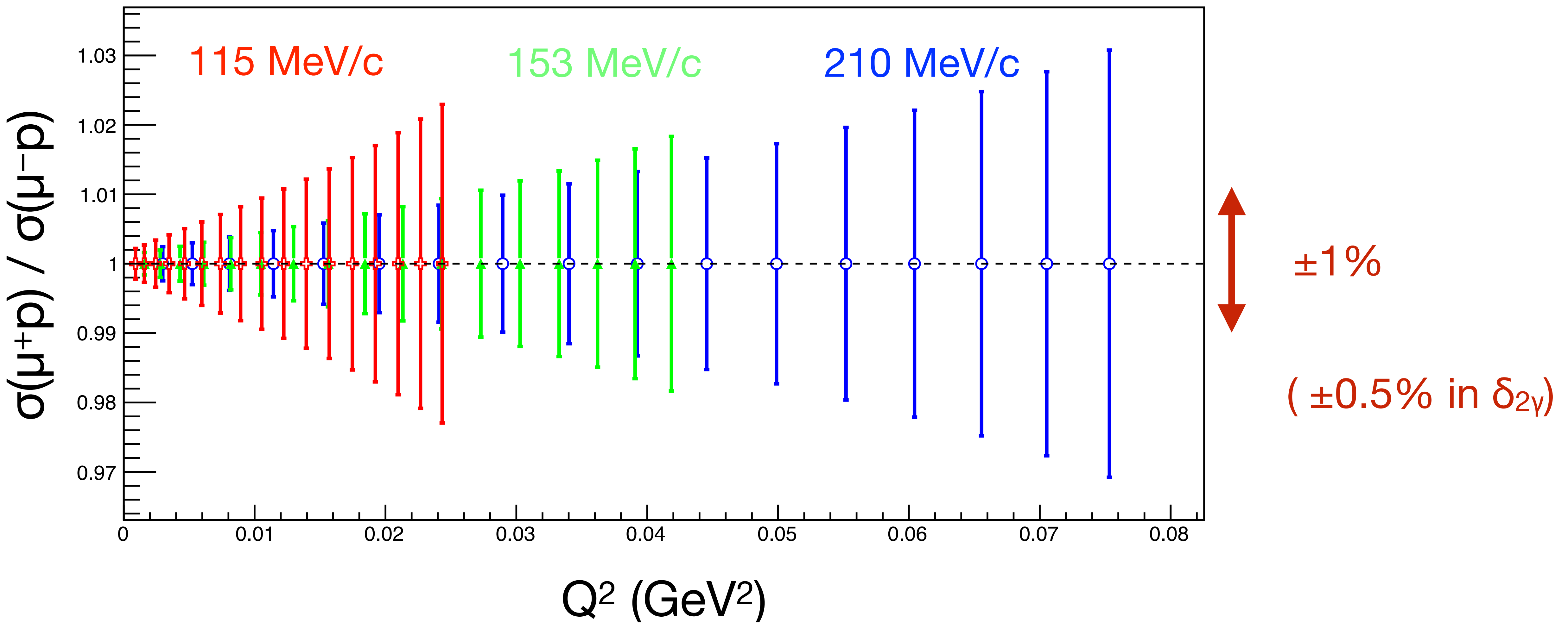

TPE correction at leading order, $\delta_{2\gamma}$

$$\sigma^{\pm} = \sigma_{1\gamma}(1 \pm \delta_{2\gamma})$$

$$\frac{\sigma^+}{\sigma^-} \approx 1 + 2\delta_{2\gamma}$$

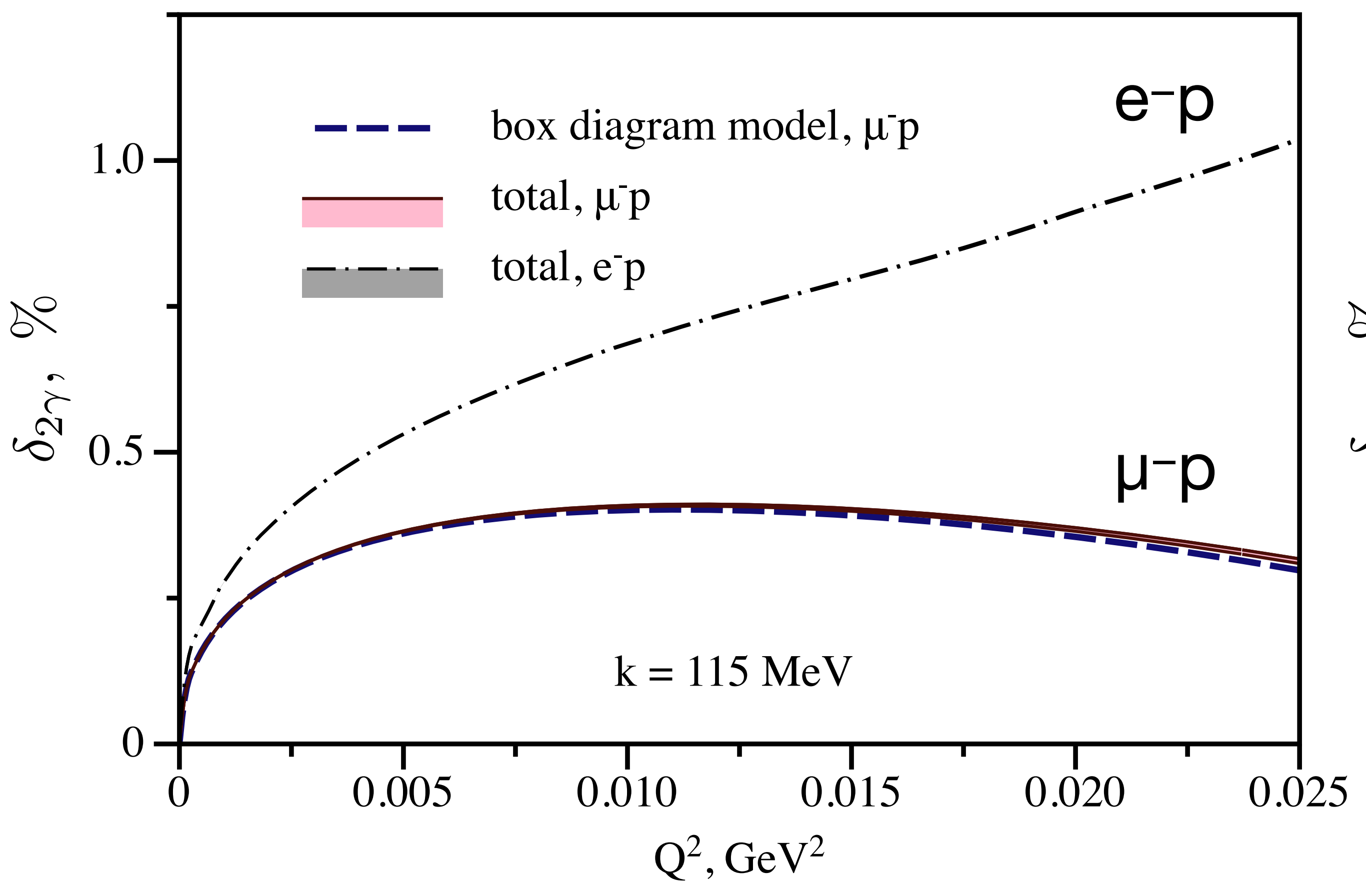

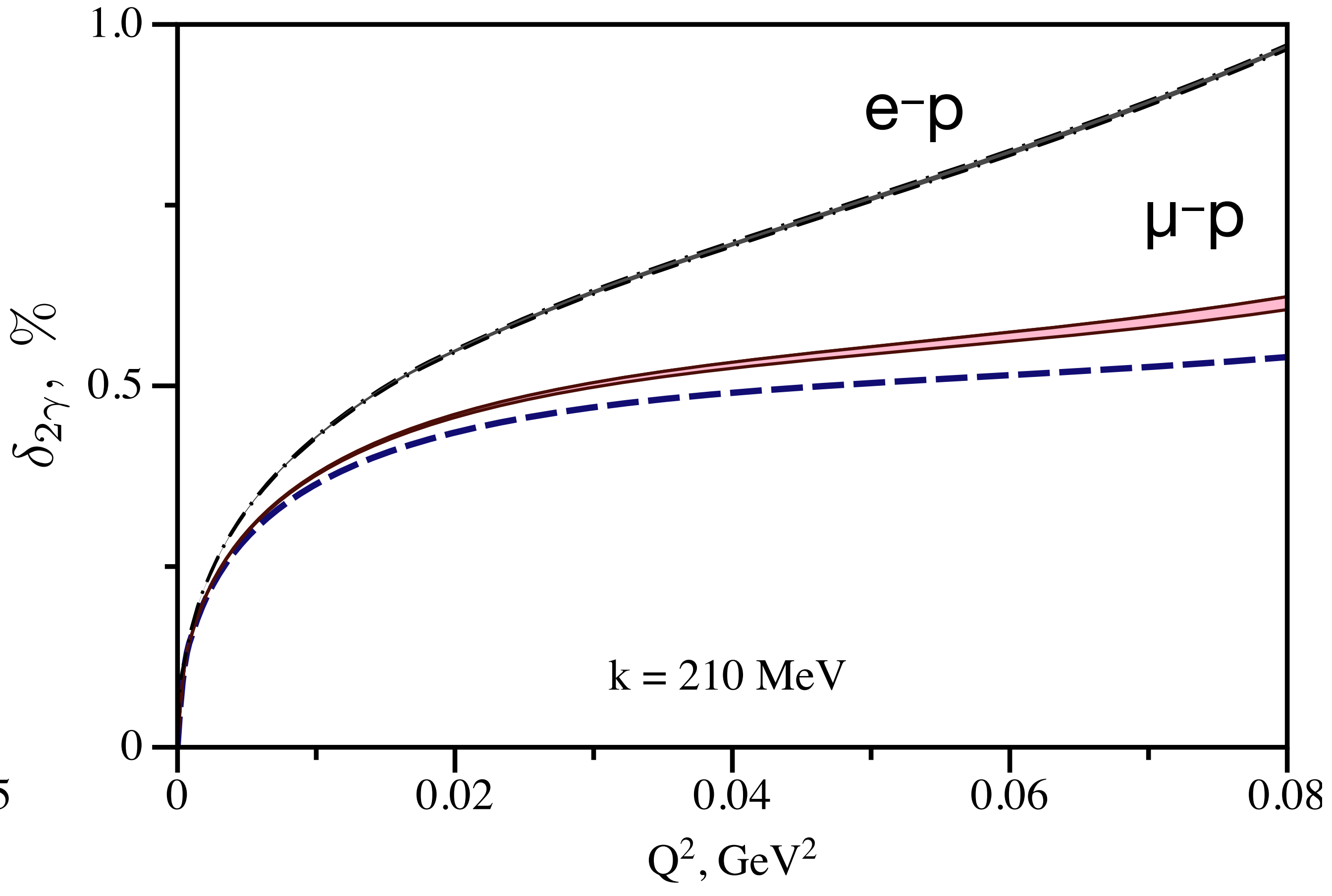

Prediction: Due to the cancellation of the helicity-flip and non-flip contributions, TPE in μp smaller than in ep.

Oleksandr Tomalak, Few-Body Systems, **59**, 87 (2018)

MUSE at the secondary beam line πM1

Beam

- 50 MHz RF (20 ns bunch separation)
- e, μ, π beams with large emittance
- Flux: 3.3 MHz
- Momentum: 115, 160, 210 MeV/c

Beam line detectors:

- Timing, identifying, and tracking of beam particles to the target and beyond

Scattered particle detectors:

- Timing and tracking of scattered particles with large solid-angle coverage

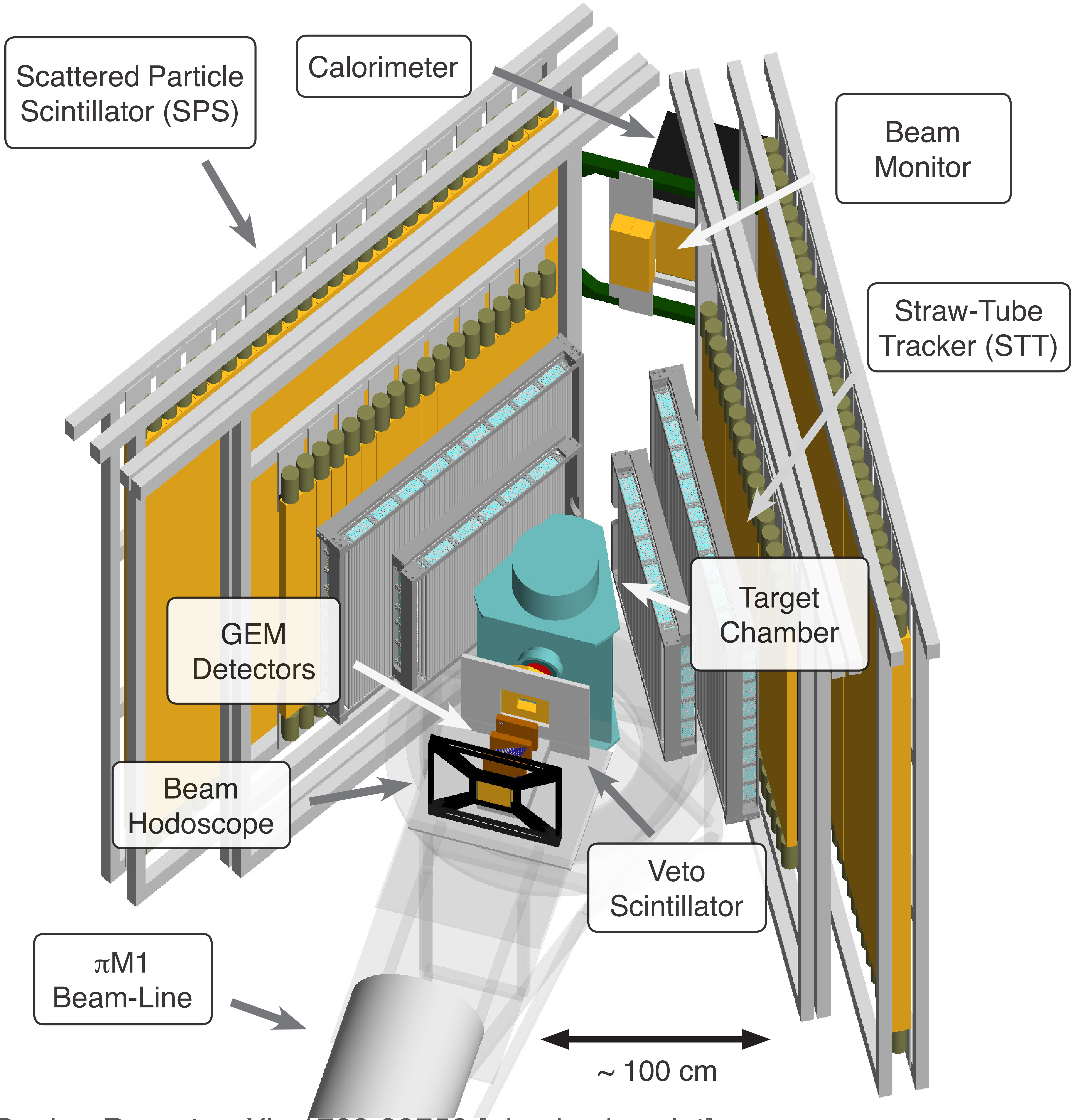

The MUon Scattering Experiment at PSI (MUSE), MUSE Technical Design Report, arXiv:1709.09753 [physics.ins-det]
E. Cline et al. (MUSE Collaboration), Phys. Rev. C 105 (2022) 5, 055201.

Radiative corrections needed to obtain Born cross-section

Experimental Bremsstrahlung cross-section

$$\frac{d\sigma^{exp}}{d\Omega_l}(p'_{l,min}) = \int_{p'_l}\int_{\Omega_\gamma} \frac{d\sigma_{\text{brems}}}{d\Omega_l d\Omega_\gamma dp'_l} d\Omega_\gamma dp'_l$$

Born cross-section

$$\frac{d\sigma^{exp}}{d\Omega_l}(p'_{l,min}) = \frac{d\sigma_0}{d\Omega_l}\left[1 + \delta(p'_{l,min})\right]$$

e.g.

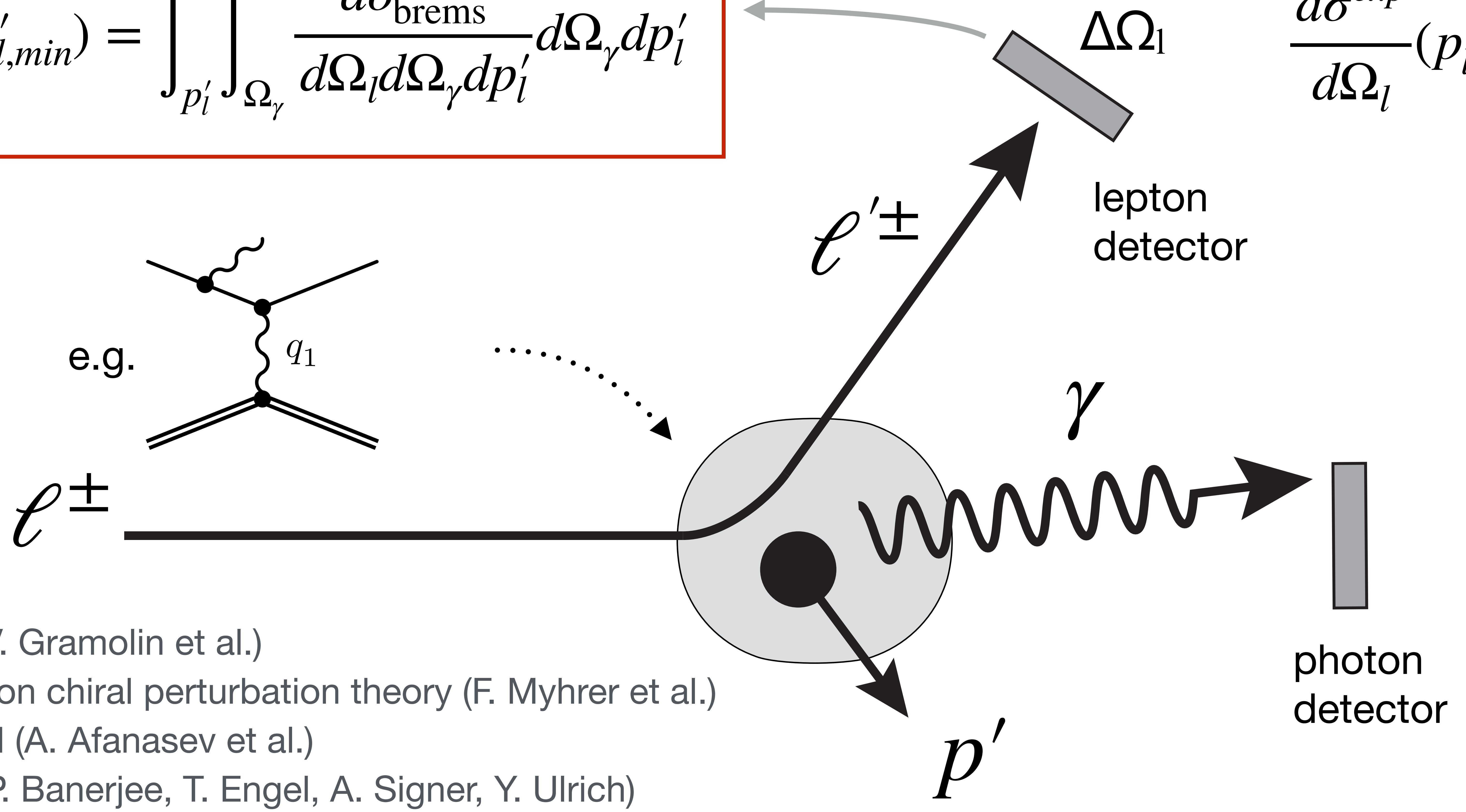

Radiative correction

$$\delta = \frac{d\sigma^{exp}}{d\Omega_l} / \frac{d\sigma_0}{d\Omega_l} - 1$$

ESEPP (A.V. Gramolin et al.)
Heavy baryon chiral perturbation theory (F. Myhrer et al.)
ELRADGEN (A. Afanasev et al.)
McMULE (P. Banerjee, T. Engel, A. Signer, Y. Ulrich)
…

Beam Hodoscope

The beam hodoscope counts the total incident beam **flux** and provides precise **timing** and **position** information for beam particles:

- RF time to hodoscope: beam-particle ID;
- Hodoscope to beam monitor: confirmation of beam-particle ID, background identification, muon and pion beam momenta, $dp/p \lesssim 0.2\%$;
- Hodoscope to scattered-particle scintillator: reaction type.

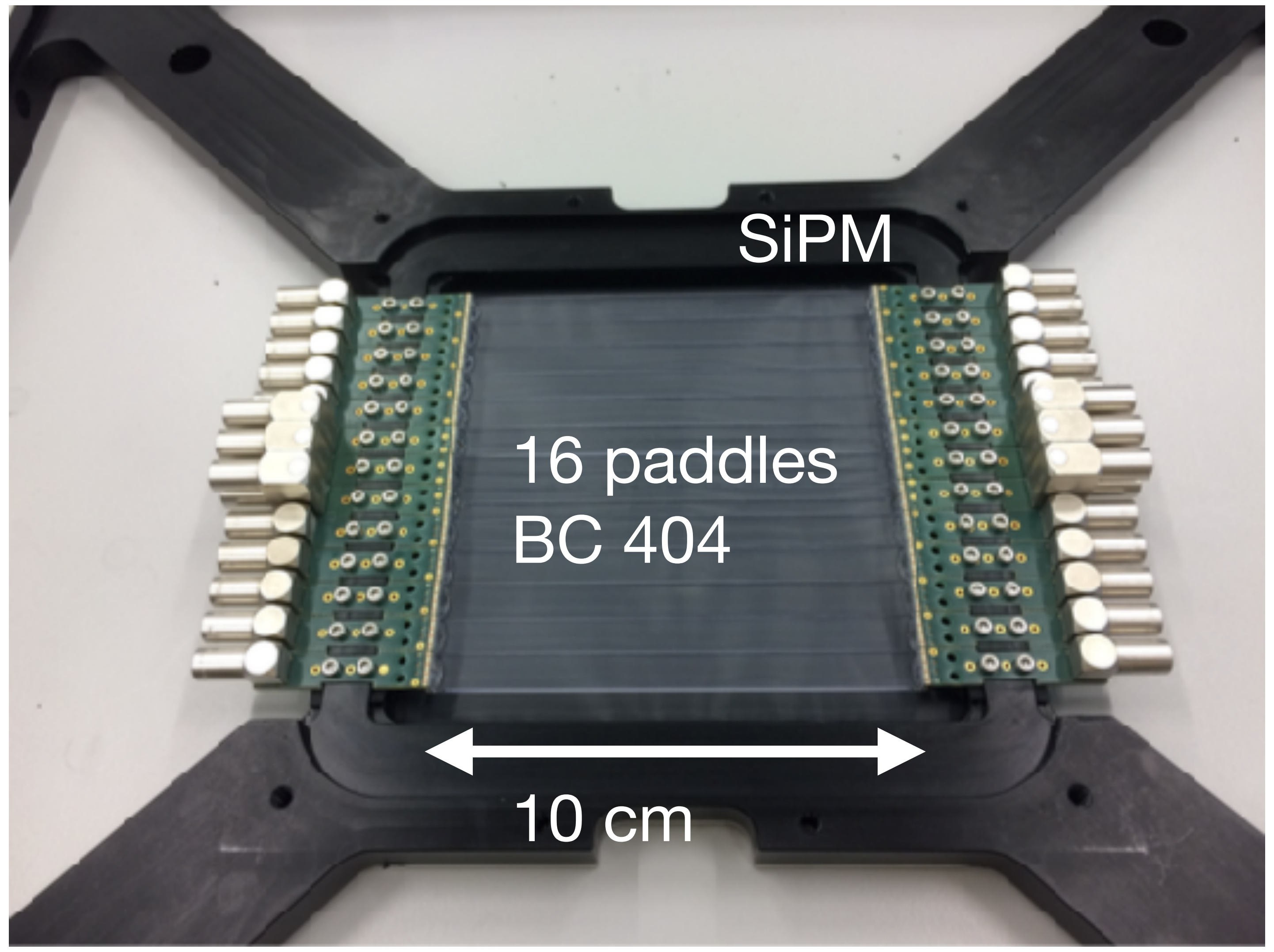

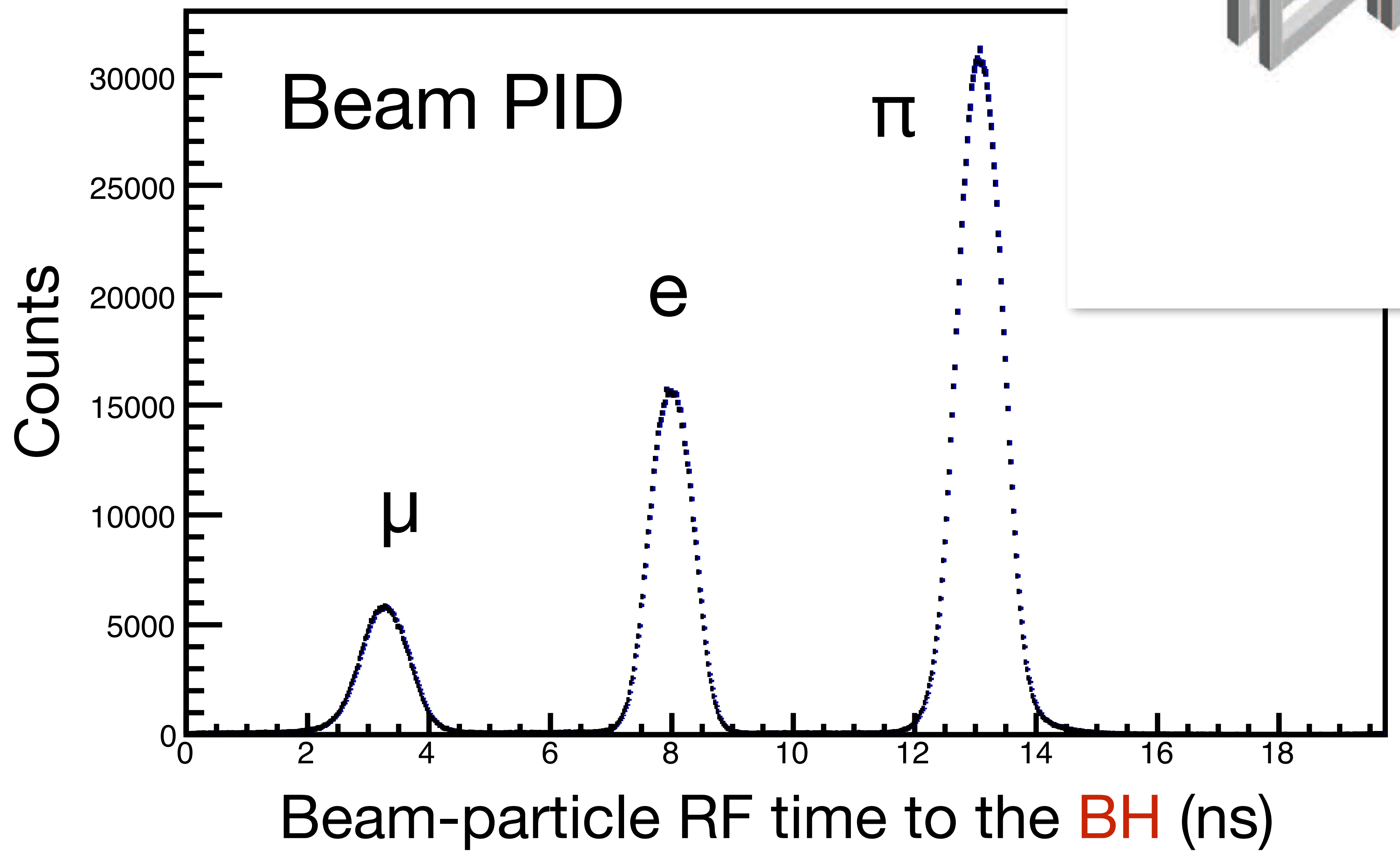

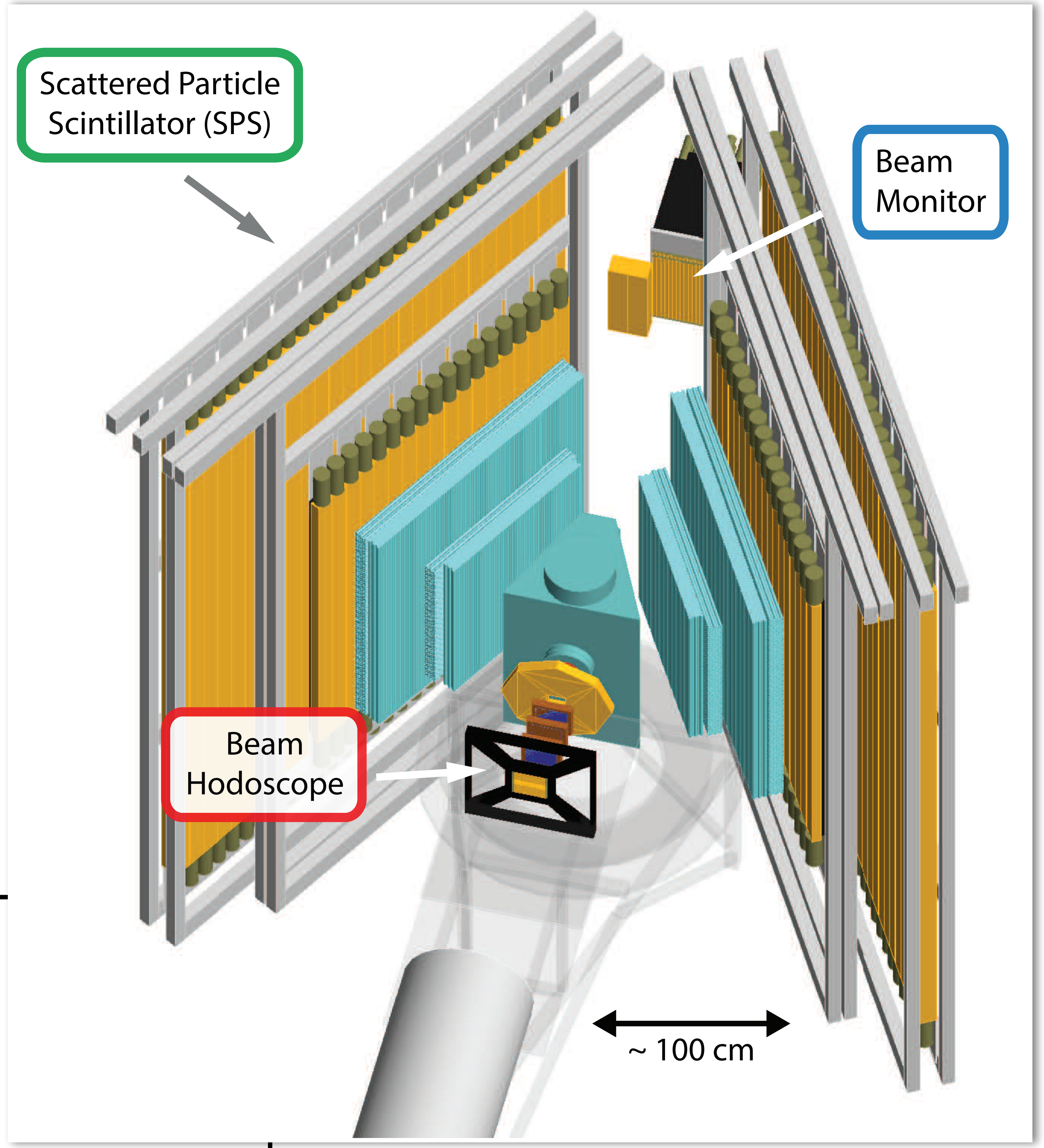

20 ns bunch separation

T. Rostomyan et al., NIM A 986, 164801 (2021)

Target and Scattering Chamber

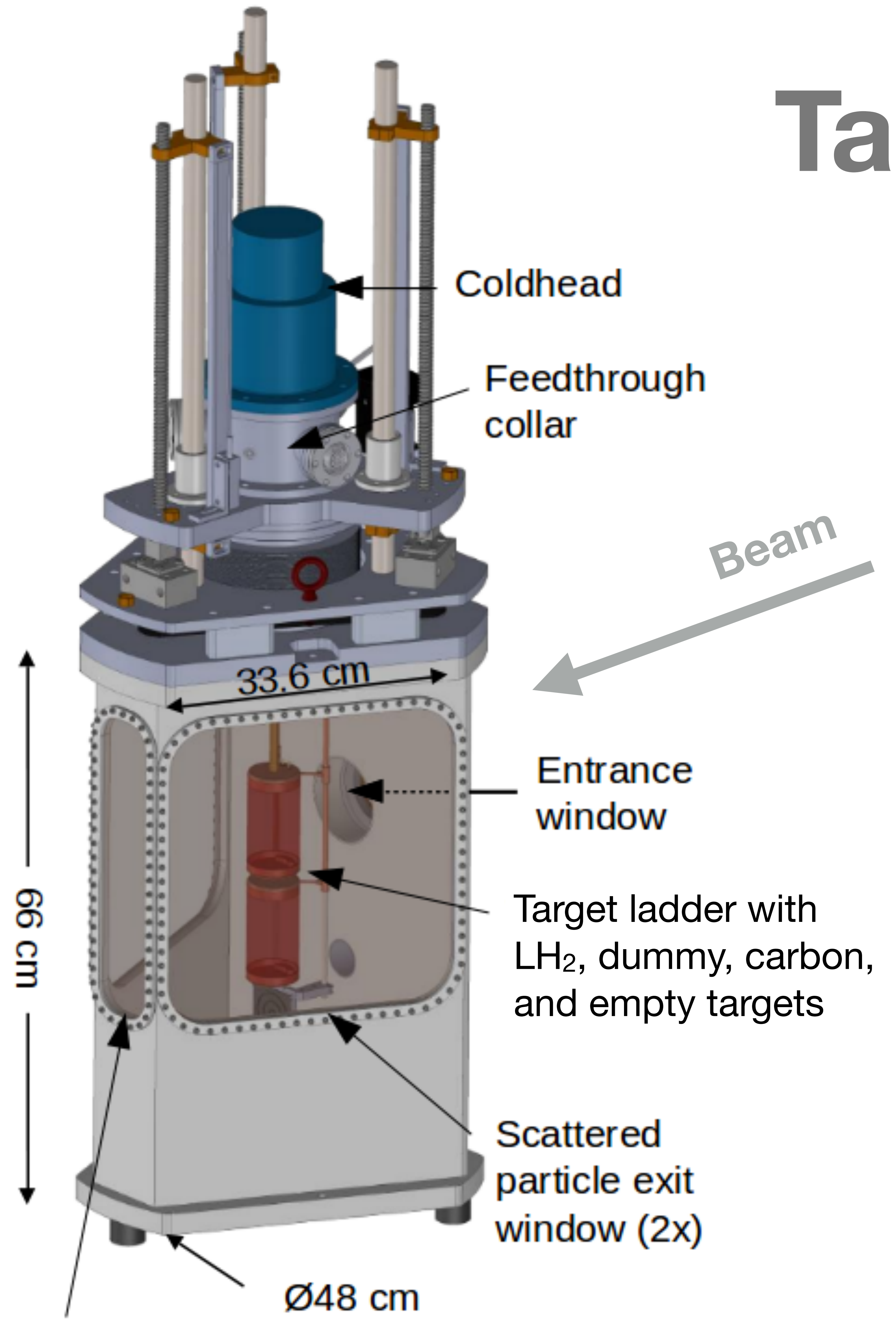

Roy et al., NIM A949, 162874 (2020)

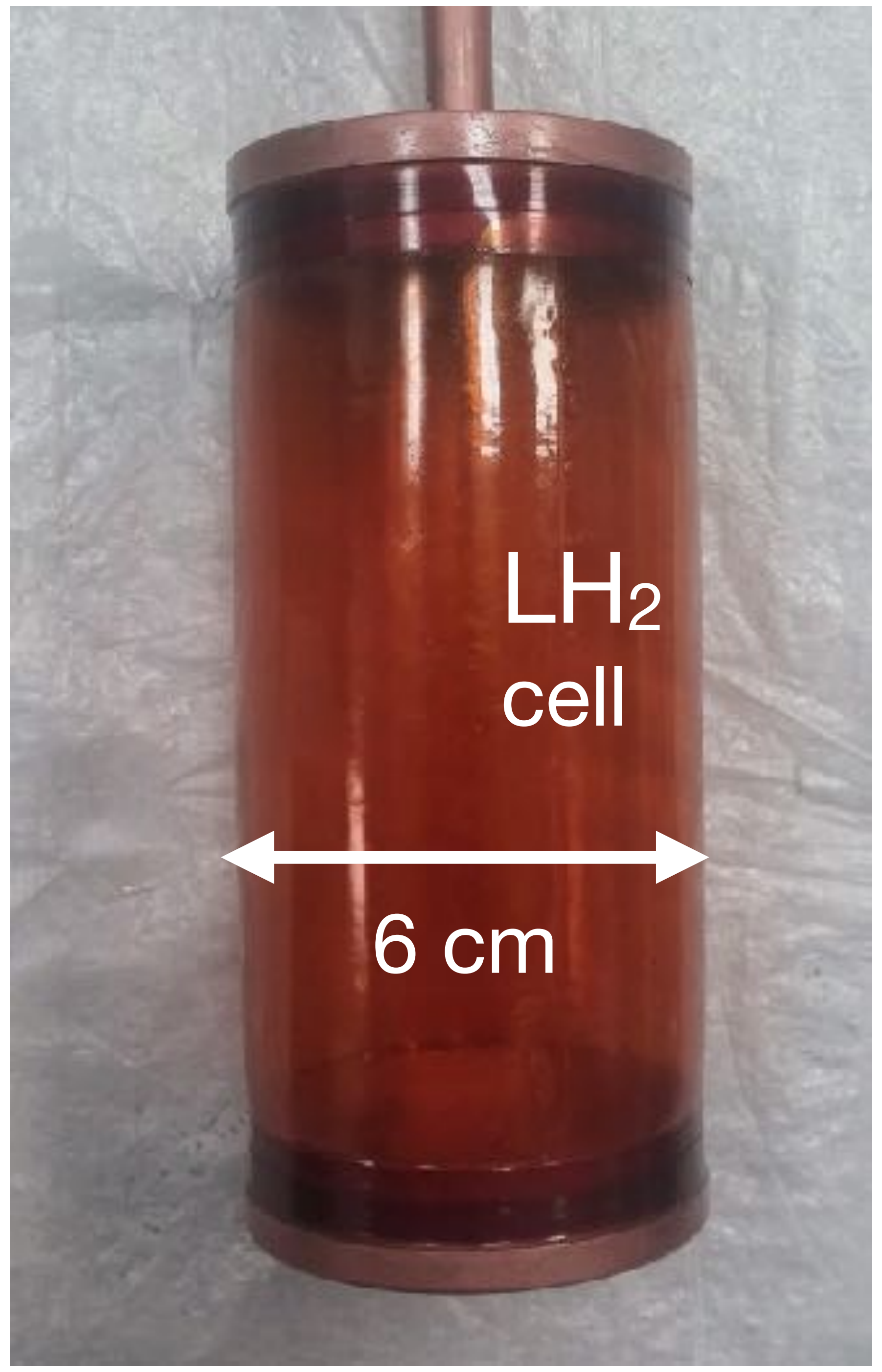

LH_2 target cell

Target performance over 562 h

- LH_2 temperature: 20.68 ± 0.01 K
- LH_2 density: 0.070 g/cm^3 stable to 0.02%

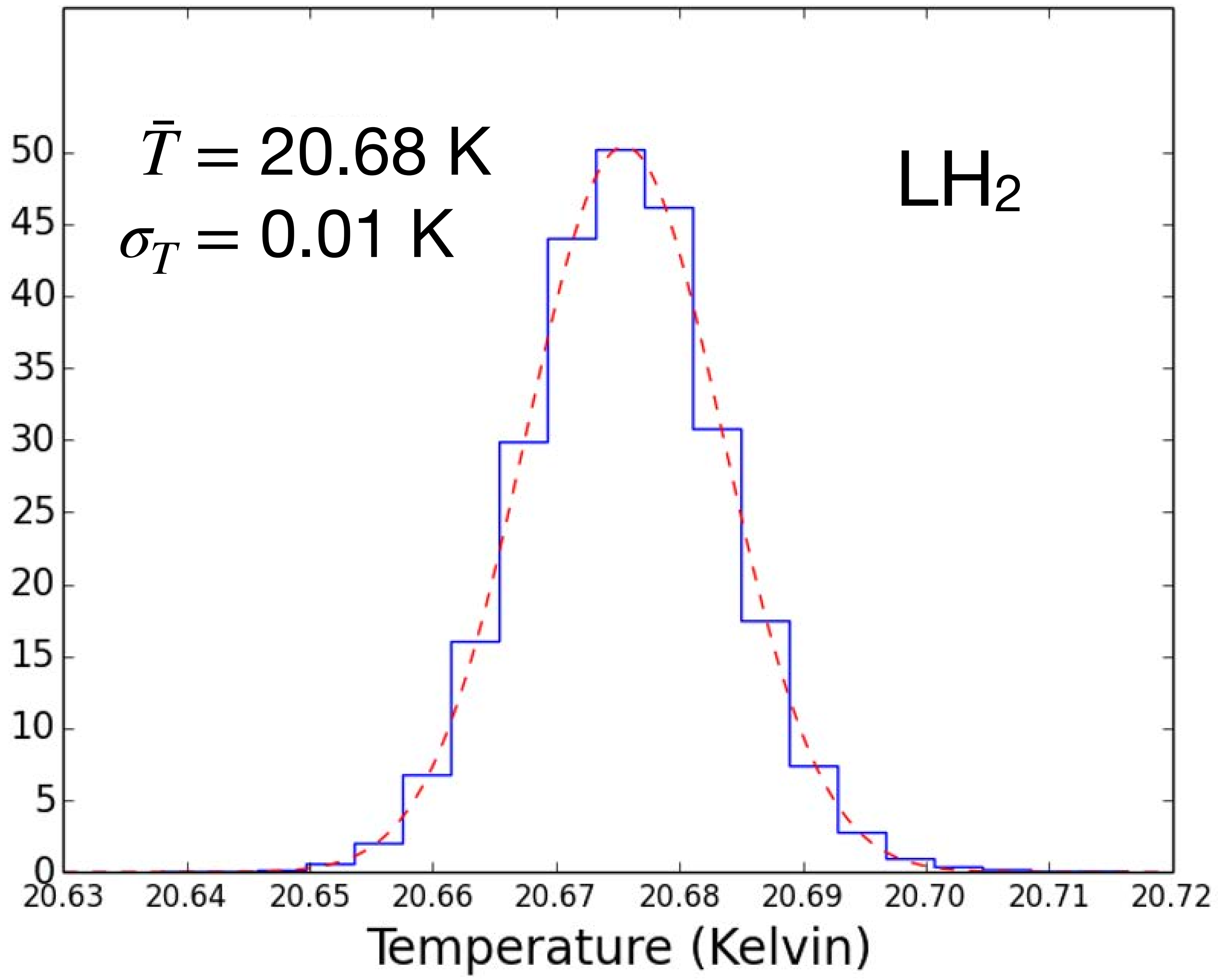

MUSE tracking detectors

GEM detectors

- Set of three GEM detectors.
- Measure trajectories into the target to reconstruct the scattering kinematics.

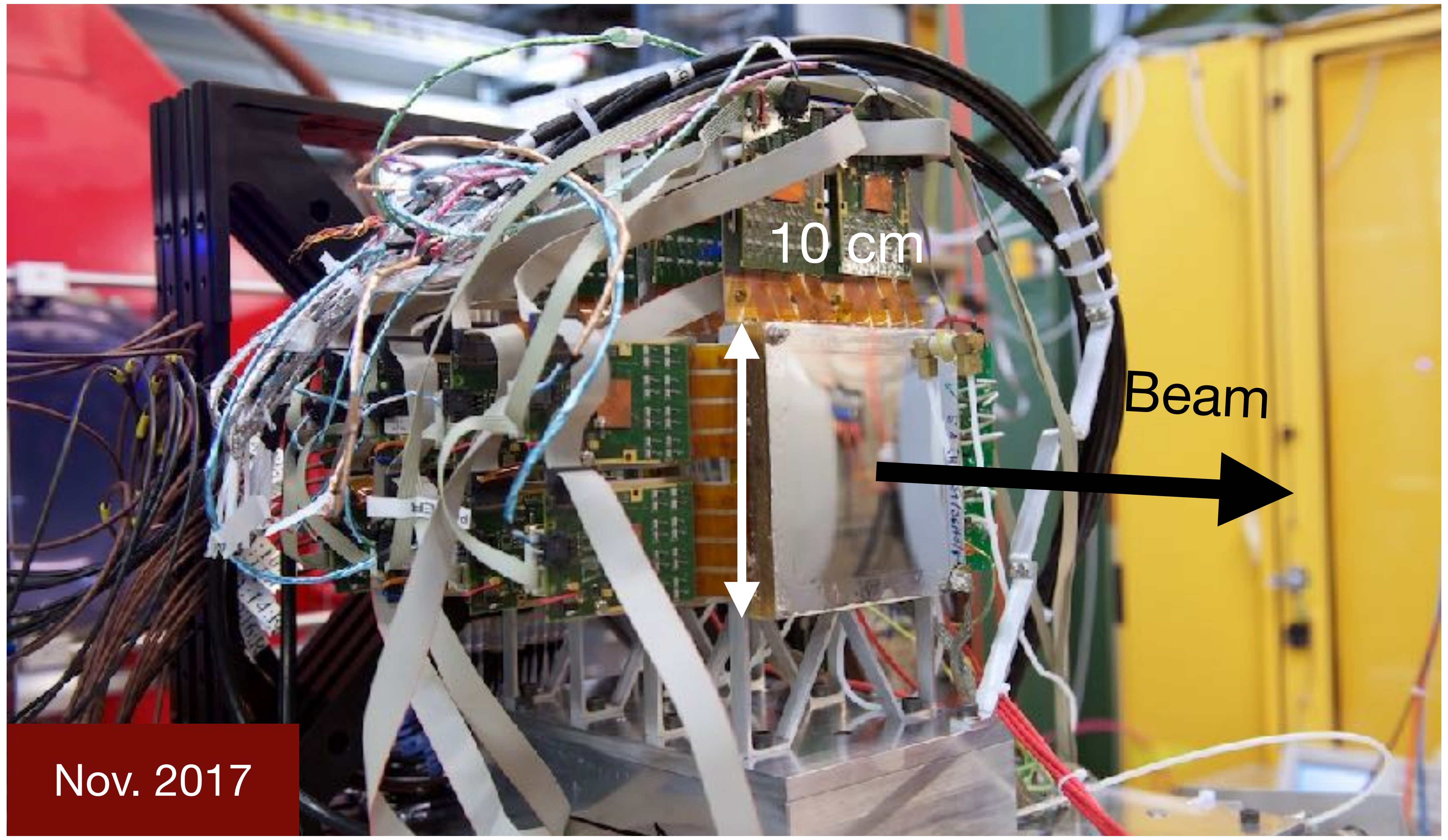

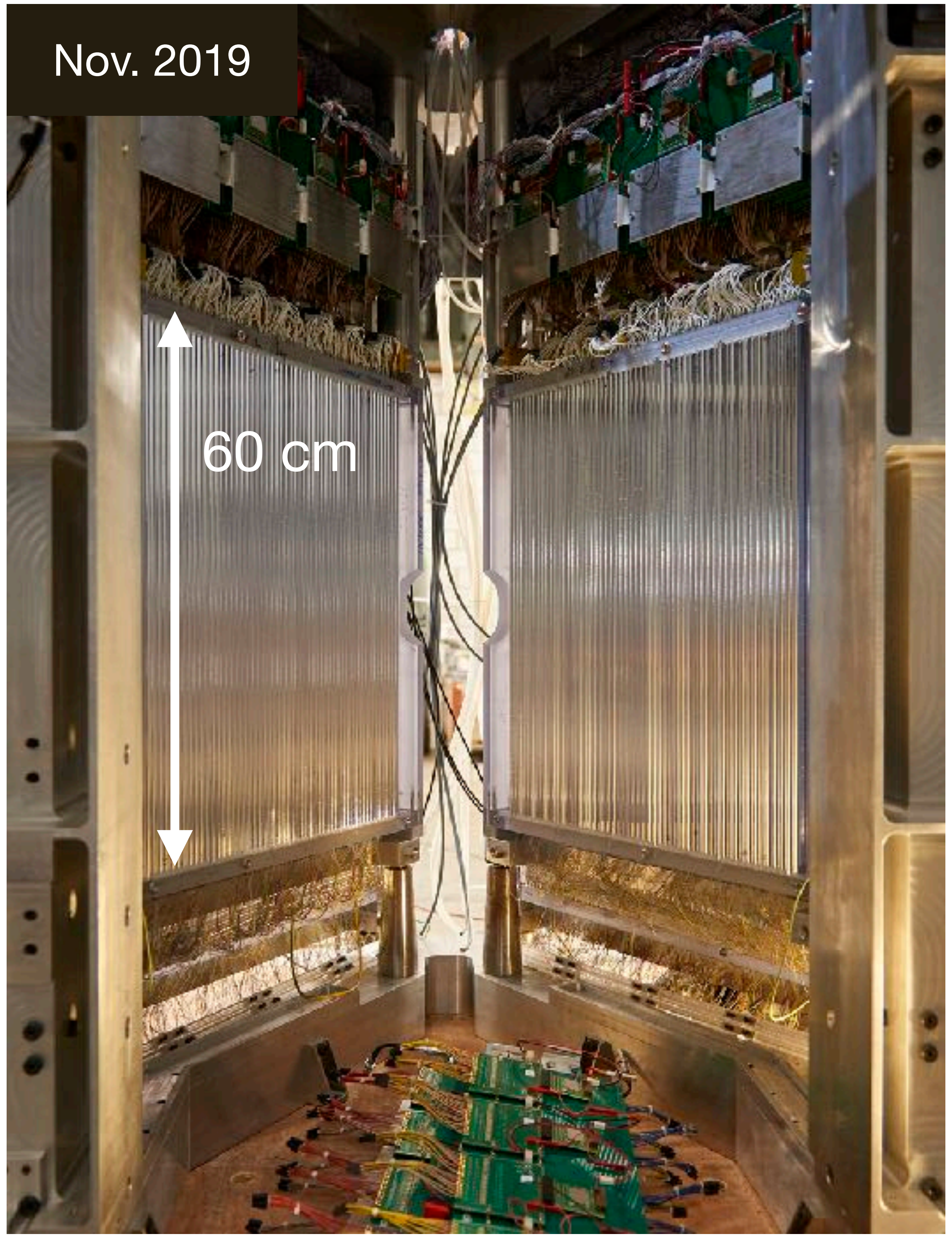

Straw-tube tracker

- Two chambers on both sides of the beamline with 5 vertical and 5 horizontal planes each (3000 straws total).
- The Straw Tube Tracker provides high-resolution and high-efficiency tracking of the scattered particles from the target.

Scattered-particle scintillators as event trigger and for reaction ID

Front wall: 18 bars (6 cm x 3 cm x 120 cm)
Rear wall: 28 bars (6 cm x 6 cm x 220 cm)

Scattered-particle scintillators exceed required time resolution:

σ(Front) < 50 ps, σ(Rear) < 60 ps

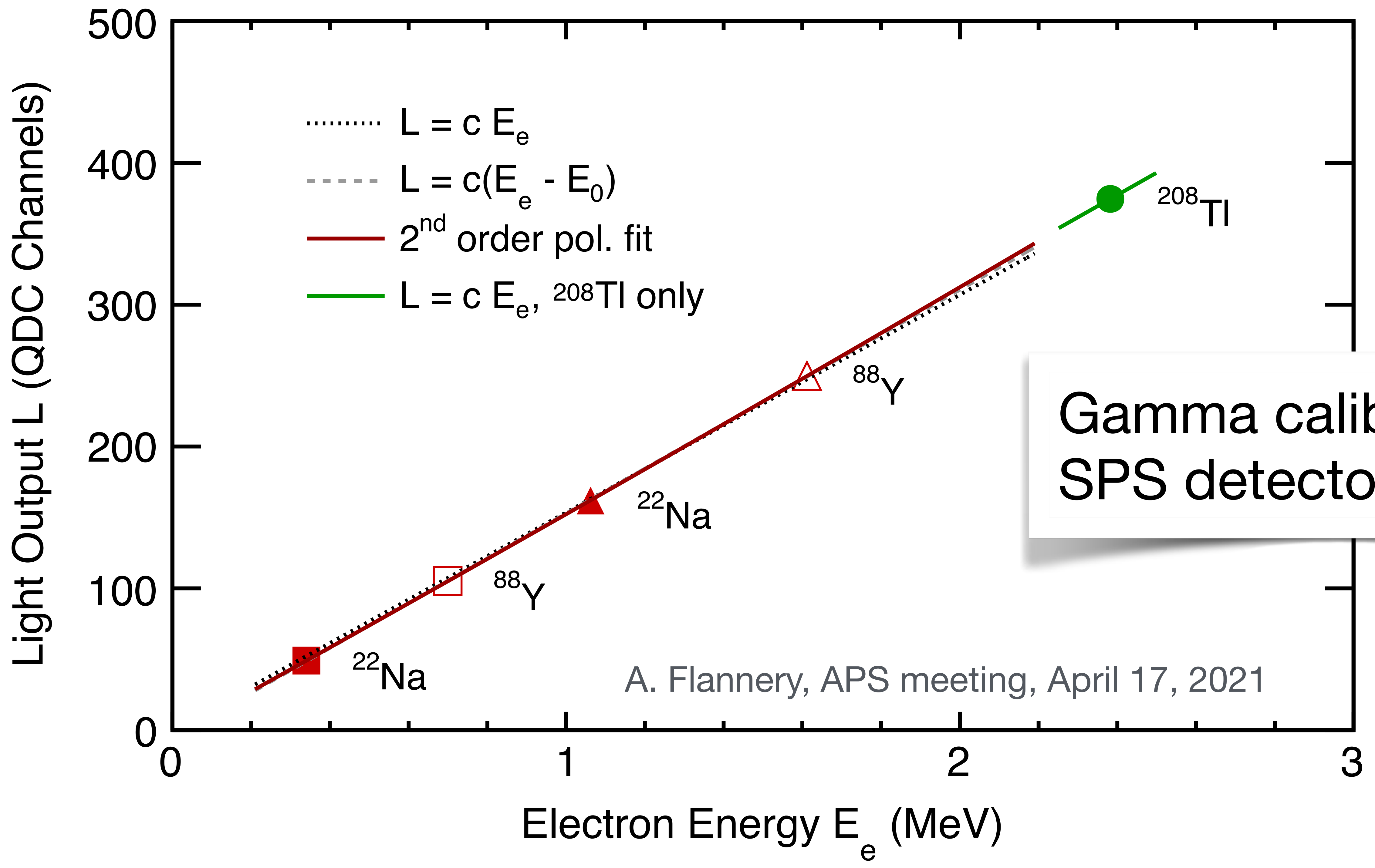

Gamma calibration of SPS detectors

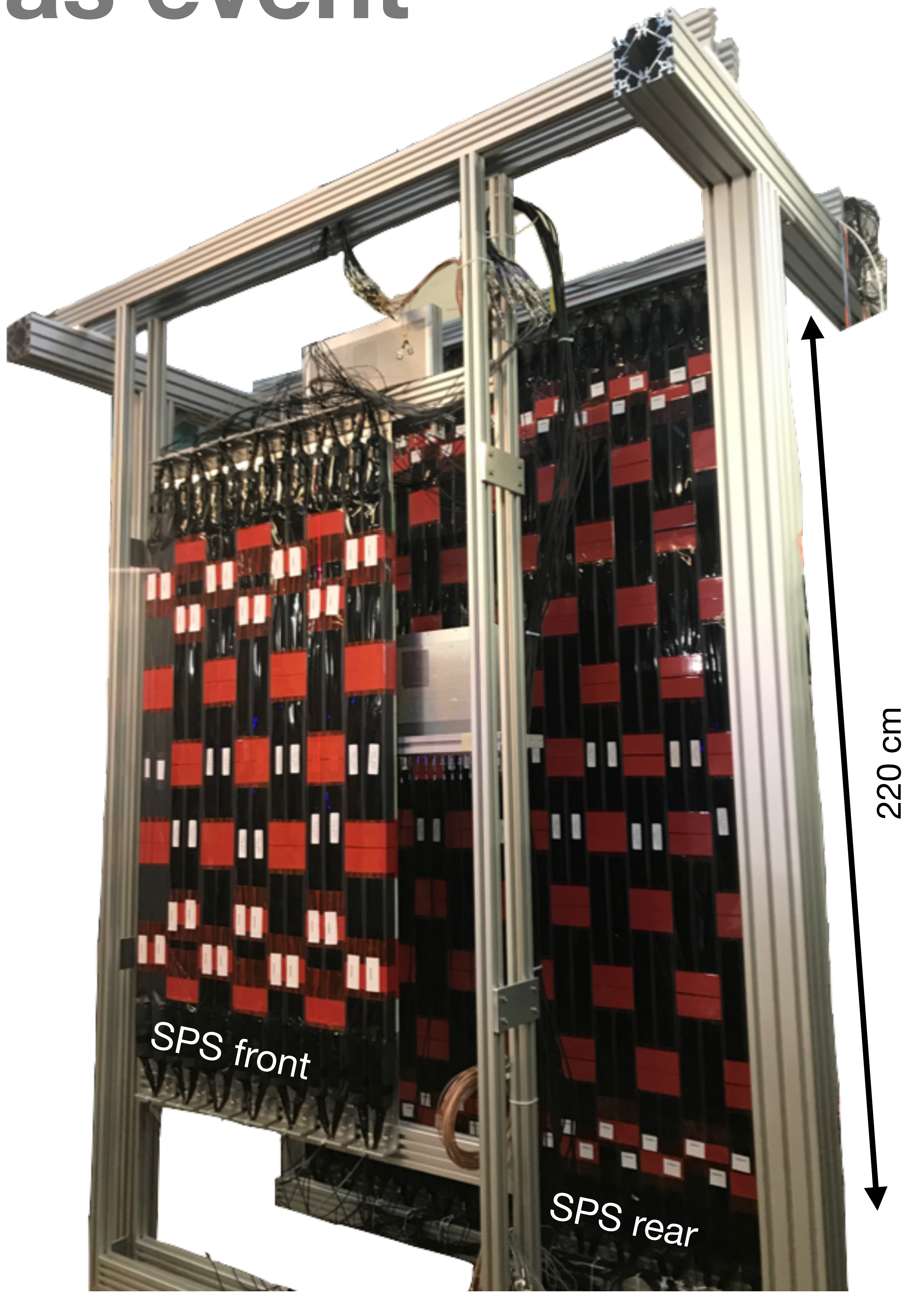

SPS detector in test stand

p'$_{min}$ is primarily determined by the SPS detector

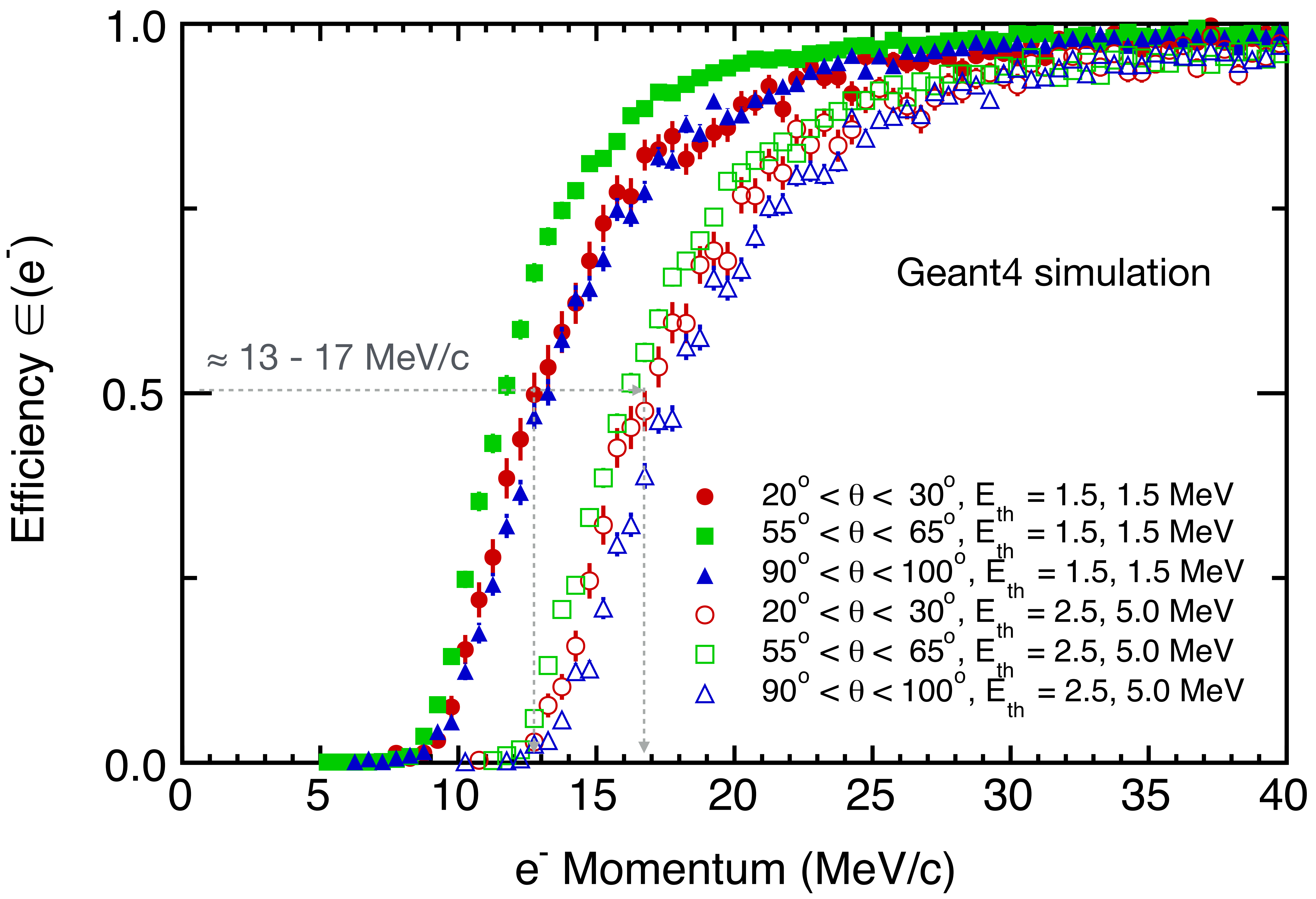

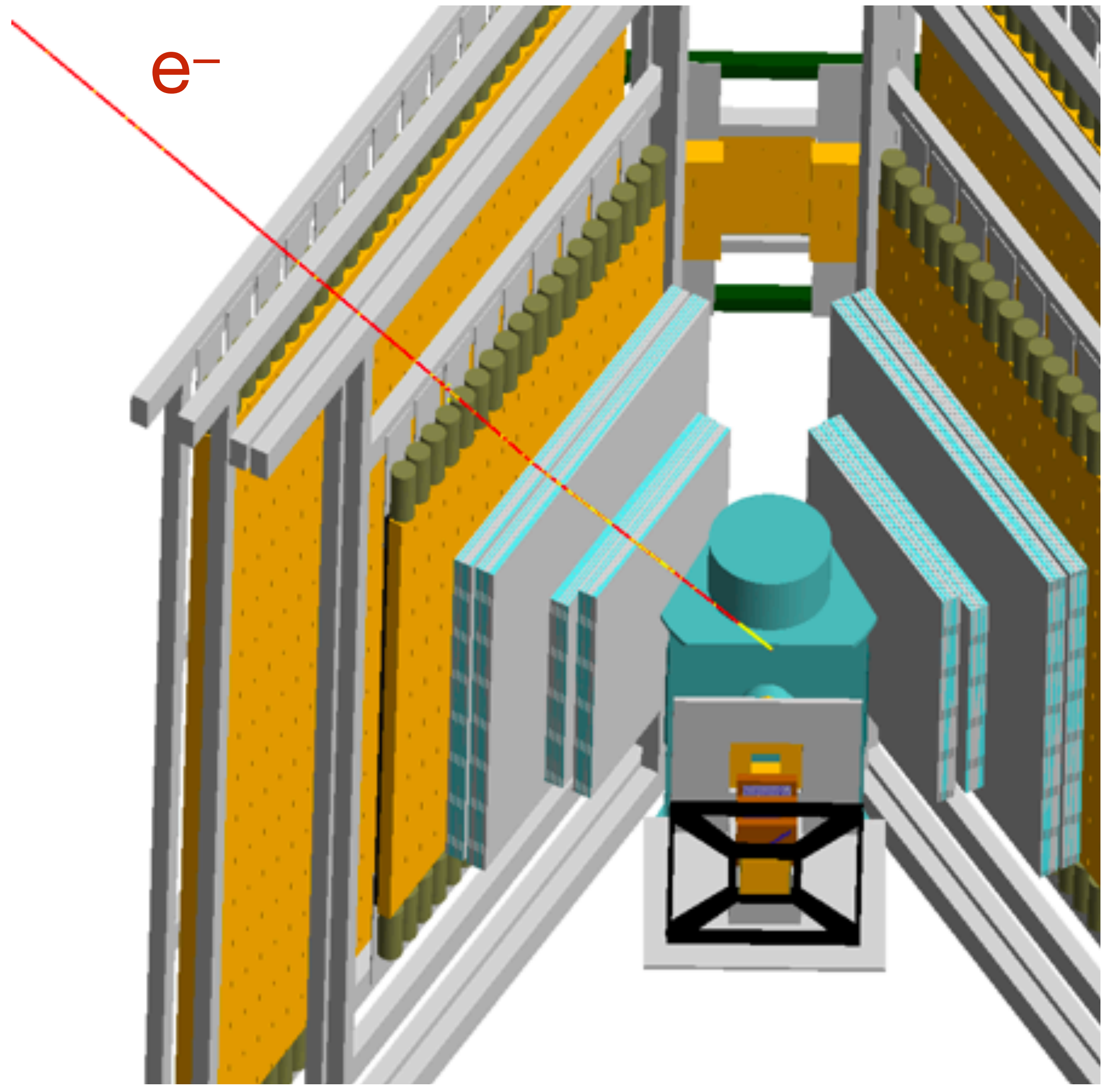

- Function of the SPS **thresholds** in the front and rear walls
- Function of the lepton **scattering angle**

$ep \to e'p\gamma$ Cross section in MUSE kinematics

MUSE will integrate over a large momentum range

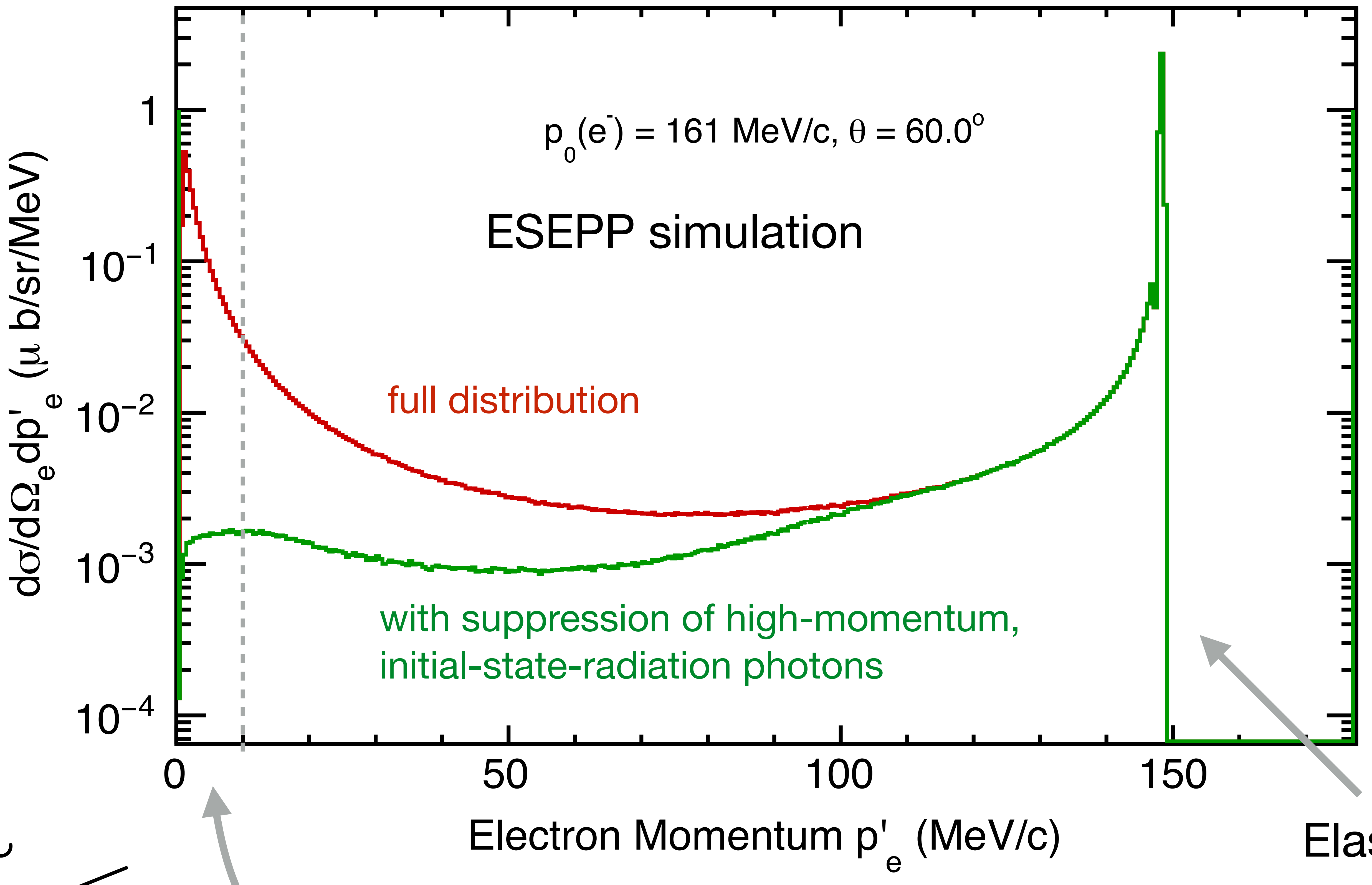

Elastic peak

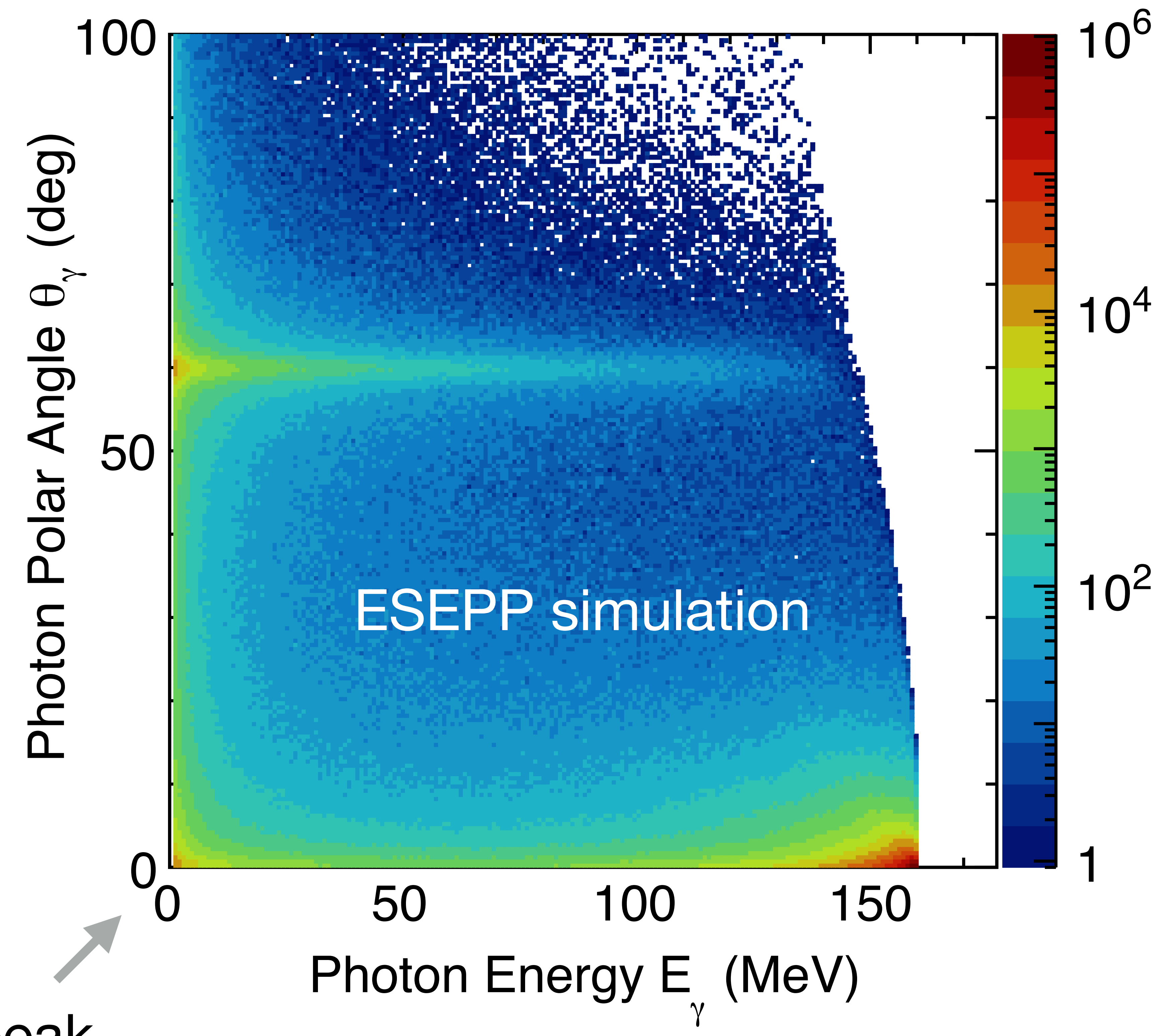

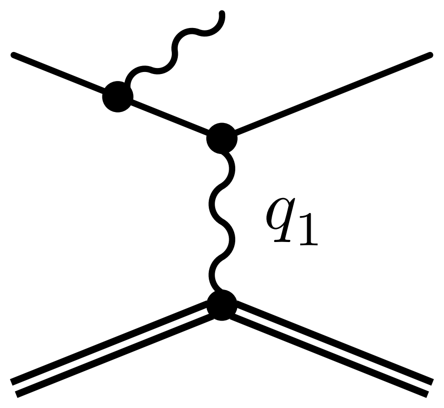

If the incident lepton loses energy due to the emission of a hard photon, then the probability for this lepton to be scattered by the proton increases.

The downstream photon calorimeter will veto events with hard initial-state radiation

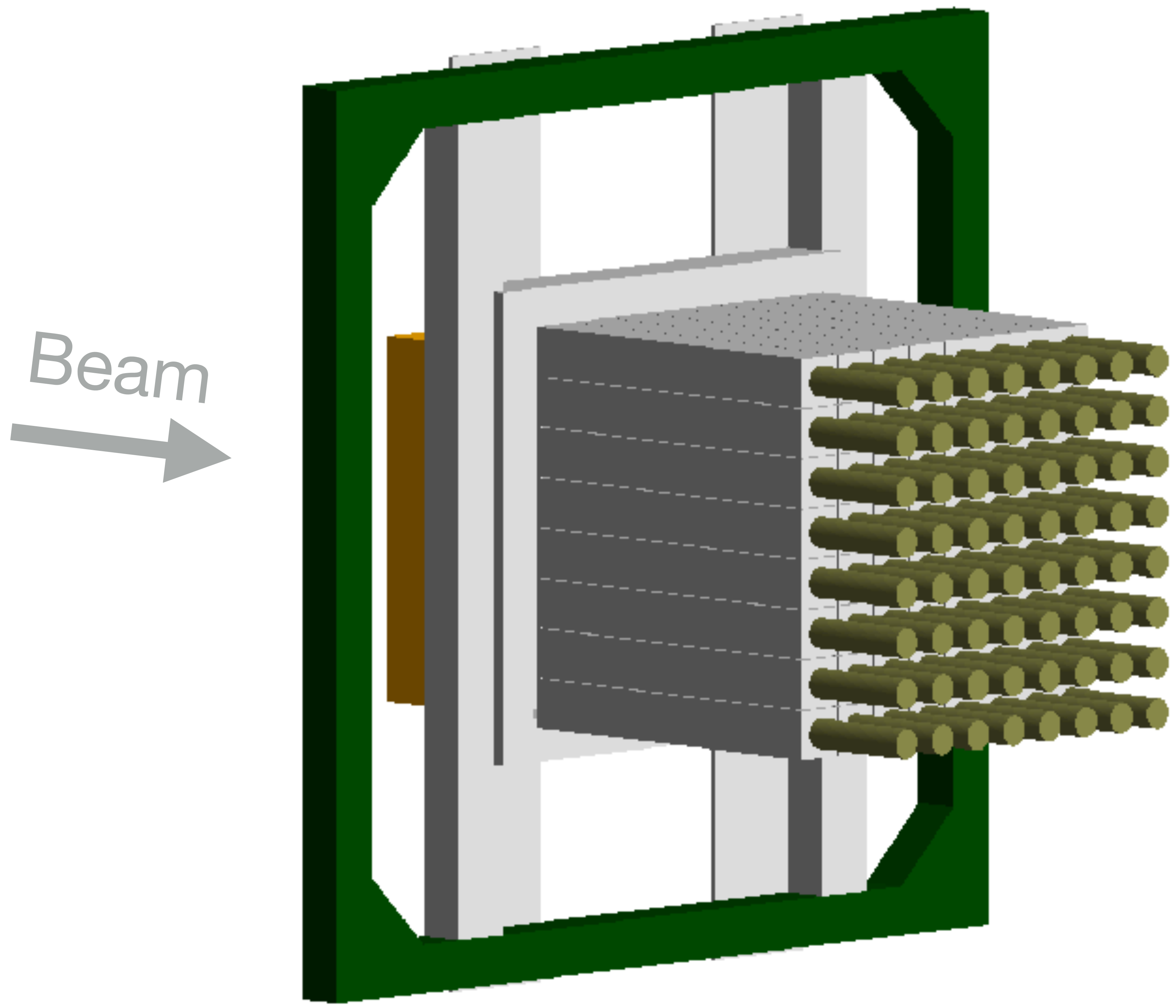

64 lead-glass crystals
(4 cm x 4 cm x 30 cm)

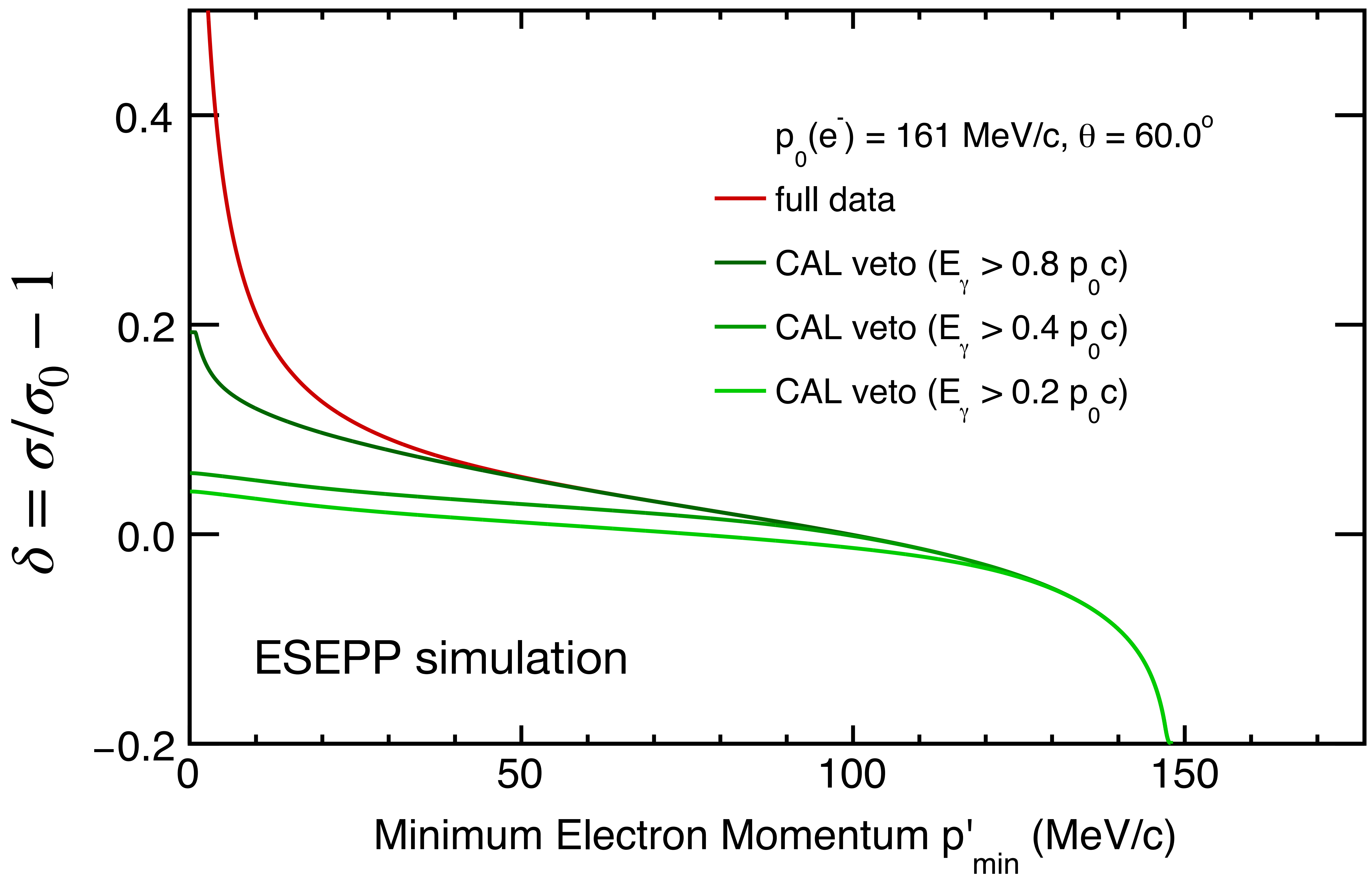

Rapidly changing radiative corrections for small p'_{min}.

(> 1% change / MeV/c)

CAL veto on downstream photons reduces radiative corrections and p'_{min} dependence, reducing uncertainty.

Lin Li, Ph.D. thesis, UofSC 2022

Uncertainties in the radiative corrections

- The preliminary estimates of the total uncertainties in the radiative corrections for **electrons** are 0.2% - 0.5%.*

$\sigma_\delta(e^-)$	115 MeV/c			161 MeV/c			210 MeV/c		
	20°	60°	100°	20°	60°	100°	20°	60°	100°
p'_{min}	0.05%	0.18%	0.30%	0.03%	0.16%	0.31%	0.02%	0.13%	0.31%
θ	0.01%	0.01%	0.00%	0.01%	0.00%	0.00%	0.00%	0.03%	0.01%
p_0	0.00%	0.00%	0.00%	0.00%	0.00%	0.00%	0.00%	0.00%	0.00%
E_γ	0.32%	0.33%	0.33%	0.25%	0.25%	0.26%	0.20%	0.22%	0.22%
Total	**0.32%**	**0.38%**	**0.45%**	**0.25%**	**0.30%**	**0.40%**	**0.20%**	**0.26%**	**0.38%**

angle-dependent uncertainty, relevant for radius extraction, $\lesssim$ 0.3%

angle-**in**dependent uncertainty, **not** relevant for radius extraction

- The preliminary estimates of the total uncertainties in the radiative corrections for **muons** are smaller than 0.01%.*

* Not including model uncertainties.

Summary and Outlook

- **MUSE** measures $\mu^{\pm}p$ and $e^{\pm}p$ scattering cross sections and will directly compare μp and ep interactions, extract the proton charge radius, and study two-photon exchange effects.

- Radiative corrections of electron-scattering cross sections are a leading source of systematic uncertainties in the experiment.

- A dedicated downstream photon detector helps to suppress initial-state radiation effects, and simulations show angular-dependent uncertainties in radiative corrections to the electron cross section be up to 0.3%.

- The collaboration is presently taking scattering data.